Available online at www.sciencedirect.com
ScienceDirect
Journal of Magnetic Resonance 190 (2008) 307–315
JMR Journal of Magnetic Resonance
www.elsevier.com/locate/jmr

Spin-labeled gel for the production of radical-free dynamic nuclear polarization enhanced molecules for NMR spectroscopy and imaging

Evan R. McCarney, Songi Han *

The Department of Chemistry and Biochemistry and The Materials Research Laboratory, University of California, Santa Barbara, CA 93106, USA

Received 27 September 2007; revised 9 November 2007
Available online 19 December 2007

Abstract

Dynamic nuclear polarization (DNP) has recently received much attention as a viable approach to enhance the sensitivity of nuclear magnetic resonance (NMR) spectroscopy and the contrast of magnetic resonance imaging (MRI), where the significantly higher electron spin polarization of stable radicals is transferred to nuclear spins. In order to apply DNP-enhanced NMR and MRI signal to biological and *in vivo* systems, it is crucial to obtain highly polarized solution samples at ambient temperatures. As stable radicals are employed as the source for the DNP polarization transfer, it is also crucial that the highly polarized sample lacks residual radical concentration because the polarized molecules will be introduced to a biological system that will be sensitive to the presence of radicals. We developed an agarose-based porous media that is covalently spin-labeled with stable radicals. The loading of solvent accessible radical is sufficiently high and their mobility approximates that in solution, which ensures high efficiency for Overhauser mechanism induced DNP without physically releasing any measurable radical into the solution. Under ambient conditions at 0.35 T magnetic field, we measure the DNP enhancement efficiency of ^{1}H signal of stagnant and continuously flowing water utilizing immobilized stable nitroxide radicals that contain two or three ESR hyperfine splitting lines and compare them to the performance of freely dissolved radicals.

Keywords: Spin label; Hyperpolarization; Hyperpolarized water; Signal amplification

1. Introduction

Much effort has been invested in the development of new methods to enhance the nuclear magnetic resonance (NMR) and imaging (MRI) signal by orders of magnitude to expand their application basis to the detection of low amplitude species. Dynamic Nuclear Polarization (DNP) is a prominent mechanism to achieve non-equilibrium nuclear spin polarization utilizing higher-energy unpaired electron spins, *e.g.* from stable radicals, as the polarization source [1–4]. For biological and *in vivo* DNP applications, it is crucial to obtain highly polarized samples in the fluid phase and to eliminate the radicals from the polarized samples prior to injection or detection. Here we present an affinity chromatography media, spin-labeled via stable amide bonds, that disperses the stable nitroxide radicals in high concentration with high mobility to ensure efficient DNP enhancement, while prohibiting radical release into the polarized sample. We investigated naturally abundant as well as ^{15}N and deuterium isotopically enriched 2,2,6,6-tetramethylpypiridine-1-oxyl (TEMPO) radicals, where the significantly narrower electron spin resonance (ESR) lines of the deuterium and ^{15}N-substituted nitroxide radicals are easier to saturate and provide higher DNP enhancement at lower irradiation power. The efficiency of achieving high DNP enhancement under ambient biological conditions is studied for static as well as flowing water at 0.35 T. Ultimately, we establish the ideal characteristics of a polarization matrix that would provide the maximum

* Corresponding author. Fax: +1 (805) 893 4120.
E-mail address: songi@chem.ucsb.edu (S. Han).

1090-7807/$ - see front matter © 2007 Elsevier Inc. All rights reserved.
doi:10.1016/j.jmr.2007.11.013

attainable DNP enhancement while providing radical-free samples.

Highly polarized fluid samples have been obtained by two different approaches: the direct polarization of fluids and the polarization of frozen samples and subsequent quick melting. The former mechanism, the Overhauser effect, is an established technique with the first experiments dating back decades [1,3,5–8], while the polarization of frozen samples and subsequent quick melting [9–11] is a more recent development. Here, the Overhauser effect is the only mechanism that allows for continuous flow-mode polarization as the fluids are directly polarized under ambient conditions, with the potential to realize continuous-flow polarization inside an MRI magnet for perfusion MRI monitoring [12]. Dorn et al. [6,13] have extensively studied the polarization of several flowing organic solvents using TEMPO immobilized on polymer beads and silica gel, demonstrating the potential for important new applications in catalysis and reaction monitoring. However, our investigations show that spin-labels immobilized on these solid supports are much less efficient for polarizing water in continuous-flow than the hydrophilic gels described in this paper, even though the radical loadings on the inorganic solid support can be much higher. The mechanism involving low-temperature DNP and subsequent melting requires more complex equipment and follows a much slower nuclear polarization build-up, taking minutes to hours, yet it can result in enhancements of ^{1}H, ^{13}C and ^{15}N by up to four orders of magnitude in biologically relevant solutions. For both DNP methods, eliminating the radicals from the polarized sample prior to detection is desirable for *in vivo* application, however can be a toilsome task. Golman et al. [9] successfully preserved much of the polarization by quickly dissolving polarized solid mixtures with hot water and filtering out the radicals through an ion-exchange column. The spin-labeled polarization gel that we present here can be superior for such applications because the polarized fluid only needs to be physically separated from the gel after melting, no radical traces are left in the effluent, it does not specifically remove anions or cations, and it does not lose binding capability under high salt conditions as an ion exchange matrix would.

Recently we developed a new imaging method utilizing the Overhauser mechanism named Remotely Enhanced Liquids for Image Contrast (RELIC), which hyperpolarizes water as it flows over immobilized radicals providing tracer-free water as a safe, biocompatible contrast agent for *in vivo* applications [12]. In the first RELIC experiment, we were able to demonstrate stunning MRI contrast by monitoring the flow of only 2- to 3-fold signal enhanced water. In this work we show that we can now achieve −24-fold signal enhancement in continuous-flow mode and prospectively attain −120-fold [14]. This technique will enable unprecedented contrast for applications like myocardical and brain perfusion MRI as well as other systems involving macroscopic flow phenomena.

The signal enhancement we observe comes from the transfer of electron spin polarization to the protons of water. In a system of two coupled spins, such as a proton and a free electron, the population distribution of the proton spin energy levels will depend on the population distribution of the electron spin energy levels [1,5]. Therefore, a perturbation applied to the equilibrium electron spin populations by an oscillating magnetic field induces mutual spin flips of coupled spins causing a shift in nuclear spin populations. In liquids, motion-mediated cross relaxation processes, leading to the simultaneous spin flip of an electron and a nucleus, drive the polarization transfer, while in solids, the simultaneous electron-nuclear spin flip through the absorption of radiation tuned to the electron spin magnetic transition plus or minus the nuclear spin magnetic transition ($h(\nu_s \pm \nu_I)$ presents one of the key DNP mechanisms [15].

In this work, we focus on demonstrating the efficiency of our spin labeled agarose gel for direct, continuous-flow, DNP of water following the Overhauser mechanism, which occurs in liquids. The signal enhancement, E, that can be expected is dependent on the interaction between the electron and proton, described by the coupling factor, ρ, the electron's ability to relax the proton, described by the leakage factor, f, the saturation of the electron Zeeman transition, s, and the magnetogyric ratio of the electron and proton, γ_s and γ_I, respectively [5].

$$E = 1 - \rho f s \frac{|\gamma_s|}{\gamma_I} \tag{1}$$

For protons in water, the maximum theoretical values for f and s are 1, and 0.5 for ρ, which, given the gyromagnetic constants of a free electron and proton, results in a maximum theoretical proton signal enhancement of −330. For our current system that utilizes nitroxide-based radicals for ^{1}H enhancement of water at 0.35 T, we measured ρ to be 0.18 [14], and therefore the expected maximum enhancement to be −120. The negative value of the enhancement is due to the nature of the dipolar interaction between the electron and proton, which leads to cross relaxation that inverts the nuclear spin population in the polarized state compared to the thermal equilibrium state. We assume the radical proton interaction to be predominately dipolar, because most radical solutions have been reported to be dipolar by observing a coupling factor of 0.5 for protons at the low field limit [5]. Sepharose should be sufficiently solvated to follow this trend; however small scalar interactions between the immobilized radical and bound water cannot be excluded. For radicals immobilized on silicagel, from the negative sign of the enhanced water we can state that the interaction between radical and water is dominated by the dipolar component of the coupling factor; however again, small scalar interactions may be present.

The leakage factor follows Eq. (2), where T_1 and T_{10} are the nuclear spin–lattice relaxation times in the presence and absence of radicals respectively, where k is the relaxivity

constant [16]. A high leakage factor approaching 1 is desired to achieve maximum polarization of the sample, which requires a considerable radical concentration, C (for ^{1}H polarization of water >10 mM of TEMPO approximates $f \sim 1$).

$$f = 1 - \frac{T_1}{T_{10}} = \frac{kCT_{10}}{1 + kCT_{10}} \quad (2)$$

Conversely, higher radical concentrations will lead to a shorter T_2 and T_1 lifetime of the nuclear spins, broadening valuable NMR signatures and shortening the lifetime of MRI signal. It is therefore desirable to polarize the nuclei in the presence of a high concentration of radical and then detect the enhanced signal in the absence of the radical.

The saturation factor, s, depends generally on the irradiation power, P, as following,

$$s = \frac{AP}{1 + BP} \quad (3)$$

where the constants A and B are functions of the number of hyperfine ESR lines and the efficiency of the mixing of hyperfine states [14]. The nitrogen hyperfine splitting of the unpaired electron spin states creates three or two lines depending on the isotope employed at the nitroxide, ^{14}N or ^{15}N. At first sight, one may assume that the 2-line radical leads to higher saturation compared to the 3-line radical because conventional continuous wave (cw) instrumentation only allows for the irradiation of one frequency at a time. However, at reasonably high radical concentration and high irradiation power, we observed equal saturation factors for the two or three line radicals, which is attributed to efficient mixing of hyperfine states driven by Heisenberg spin exchange and nitrogen nuclear spin relaxation [14]. Heisenberg spin exchange depends on intermolecular collisions, leading to electron spin exchange between radicals, and thus saturation transfer to nuclei with different spin states [17]. This *indirectly* allows for the saturation of all the hyperfine states while irradiating only one frequency. Nitrogen nuclear spin relaxation will *directly* mix nuclear spins through the spin–lattice relaxation of the nuclei [14]. Therefore, by increasing the radical concentration, the intermolecular collision rate will increase and lead to Heisenberg exchange. The nitrogen nuclear spin relaxation, however, depends on the tumbling rate of the nitroxide radical, given the magnetic field strength and solvent condition. This theoretical model is described in detail elsewhere and its affect is shown in the experimental section below [14].

2. Results and discussion

2.1. ESR spectra of dissolved and immobilized radicals

In order to maximize saturation (s) and thus DNP enhancement (E) with lower irradiation power at 10 GHz, we synthesized ^{15}N-perdeuterated-4-amino-TEMPO to reduce the number of hyperfine states from three to two and reduce (40%) the line widths compared to the natural abundance radical (1.2 G for ^{15}N-perdeutero- and 2.0 G for ^{14}N TEMPO at 10 mM) (Fig. 1A and B). Once the radicals are immobilized the reduction in line width is not as significant (3.8 G for ^{15}N-perdeutero- and 4.0 G for ^{14}N TEMPO), however by using ^{15}N labeled TEMPO there is still a reduction from three hyperfine states to two, which reduces the irradiation power necessary to achieve the same enhancement (Fig. 1C and D). The TEMPO immobilized on silica gel is very broad due

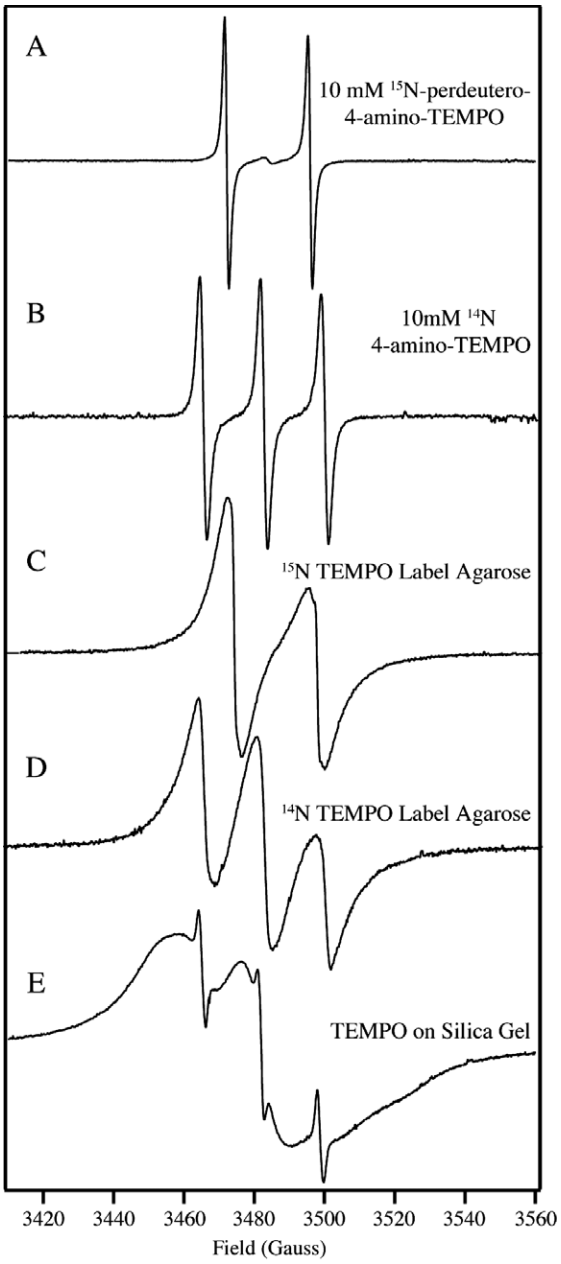

Fig. 1. Immobilization significantly broadens the ESR lines of TEMPO radicals compared to their solution state spectra. ESR spectra were acquired for dissolved TEMPO and TEMPO immobilized on agarose beads and silica gel. ^{15}N-perdeutero-TEMPO labeled agarose reduced the ESR transitions from three to two, which reduced the required microwave power necessary to saturate the transition and maximizes the enhancement.

to the very high concentration of radical (Fig. 1E). We therefore believed this would lead to difficulty saturating the ESR transitions, but as will be discussed later, we were still able to saturate these lines.

2.2. Overhauser enhancement characterization

The achieved signal enhancement, E_{actual}, projected maximum enhancement at infinite power, E_{max}, and leakage factor were determined for ^{14}N 4-amino-TEMPO and ^{15}N-d_{17}-4-amino-TEMPO dissolved and immobilized onto agarose as well as a commercially available silical gel (Table 1). E_{max} was extracted from determining E_{actual} as a function of power (P), which is the parameter modulating the saturation factor (s in Eq. (3)). E_{actual} versus P curves are displayed in Fig. 2 for ^{14}N-TEMPO labeled agarose, ^{15}N-TEMPO labeled agarose, and ^{14}N-TEMPO labeled silica gel. The ability to achieve high DNP enhancement while using significantly lower irradiation power is relevant for polarizing larger sample volumes and on-site medical applications. However, with sufficient irradiation power, we are able to reach 80% saturation for both ^{14}N and ^{15}N TEMPO labeled agarose gels, despite the different line widths.

Table 1
Enhancement parameters describing the DNP properties of dissolved and immobilized TEMPO derivatives

Matrix	E_{max} static	E_{actual} static	E_{Flow}	Leakage factor	Estimated concentration (mM)
^{14}N NHS Sepharose	-42 ± 4	-33	-24	0.90	10
^{15}N NHS Sepharose	-46 ± 5	-38	-23	0.90	10
^{15}N Solution	-120 ± 7	-117	NA	0.95	10
^{14}N Solution	-120 ± 7	-110	-42	0.95	10
Silica gel	-20 ± 5	-18	-10	0.50	900

Measurements were taken for static and flowing samples. HPLC grade water was the mobile phase for all immobilized radical samples.

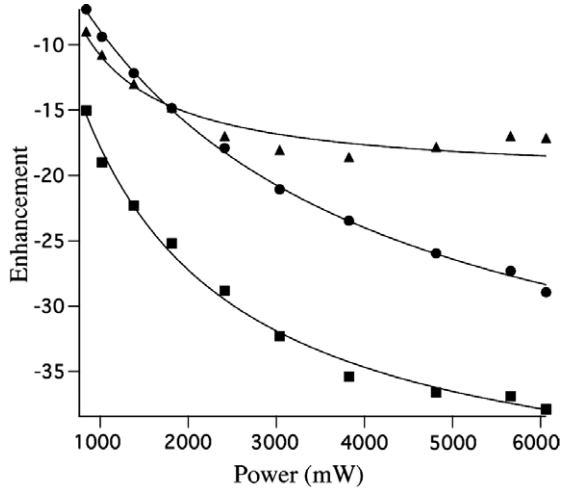

Fig. 2. The enhancement was measured as a function of microwave power for ^{14}N-TEMPO labeled agarose (circles), ^{15}N-TEMPO labeled agarose (squares), and silica gel (triangles). ^{14}N-TEMPO labeled agarose is able to enhance the ^{1}H signal of water with much less microwave power then ^{14}N-TEMPO labeled agarose. The data is fit to Eq. (5) and extrapolated out to infinite power in order to determine E_{max}.

All the enhancement parameters for ^{14}N versus ^{15}N TEMPOs dissolved as well as immobilized onto agarose are within error, which agrees with the previous discussion on the effect of nitrogen relaxation and Heisenberg exchange on the saturation factor. However, for the ^{15}N TEMPO labeled agarose gel the same amplification was reached with only 40% of the irradiation power necessary for the ^{14}N TEMPO labeled agarose (Fig. 2). This result shows that a saturation factor of unity ($s = 1$) can be reached for both isotopic states. For spin labeled agarose gels, it is unlikely that the hyperfine states mix primarily through Heisenberg exchange because the radicals are immobilized and at a sufficiently low (<10 mM) concentration to minimize inter-radical contact; therefore rapid nitrogen nuclear spin relaxation must be the cause of hyperfine mixing. This conclusion agrees with a previous study that shows that nitrogen relaxation rates are very sensitive to translational and rotational motion [18]. Here, by immobilizing the radicals on these gels, the hyperfine states are mixed through increased nitrogen nuclear spin relaxation promoted by the decreased mobility of the radicals.

The significantly smaller enhancement and leakage factor of spin labeled silica gel as compared to the spin labeled agarose gel is another interesting result (Table 1). Silica gel grains alone, without immobilized radicals, greatly reduce the T_{10} of pure water from 2.6 s to 260 ms, and therefore the silica gel-immobilized radicals have less effect in reducing T_1 of water as opposed to the effect of agarose gel-immobilized radicals on water. So, the very high radical loading of silica gel reduces the T_1 of the water only by 50%, while a lower loading of the agarose gel reduces the T_1 by >90%. This feature is manifested in the differing leakage factors, f. The reduced T_{10} in silica gel in the absence of radicals is due the effect of micropores that enhance the relaxation of water. We confirmed that the relaxation times are dependent on the pore size by measuring the T_1 of two silica gels with different pore sizes; a silica gel with smaller pores (60 Å) reduces the T_{10} to 260 ms and a silica gel with larger pores (100 Å) only reduces the T_{10} to 340 ms. So, the smaller leakage factor, f, of 0.5 as opposed to 0.9 is due to the extra modes of proton relaxation that are independent of the loaded radical; making the radicals much less effective in transferring their polarization.

The observation that the ratios between the leakage factors for agarose and silica gel samples are equal to the ratios between maximum enhancement means that the coupling factor multiplied by the saturation factor ($\rho \cdot s$) also must be equal for the two systems (Eq. (1)). Because the saturation factor for TEMPO-labeled agarose is determined to be 1 and the saturation factor for TEMPO bound

silica gel must be equal to or smaller than 1, the coupling factor for silica gel has to be equal to or greater than that of the agarose sample. Most likely the coupling factors of these materials are within error. This is in agreement with the coupling factor being a function of the distance of closest approach beween the radical and the water and the diffusion coefficient of the water near the radicals, which are unlikely to be more favorable for TEMPO bound silica gel. Therefore we predict that the coupling factor between the two samples are equal within error and the maximum saturation factor for silica gel must be equal to 1. The high saturation of TEMPO bound silica gel is probably due to both nitrogen nuclear spin relaxation as well as Heisenberg exchange, the former promoted by immobilization of the radicals and the latter by the high radical loading and efficient inter-radical contact. In conclusion, we believe that the agarose and silica gels predominately differ in respect to DNP properties by their leakage factor alone.

Overall, an important weakness of the functionalized TEMPO onto the agarose gel matrix is that the achieved ($E = -38$) as well as projected maximum enhancements ($E_{max} = -46$) are lower than with TEMPO dissolved in water at a comparable concentration. Given that our experimental results make it evident that the saturation factors (~1) as well as leakage factor (~0.9) approach 1 for both samples, we attribute the weaker DNP efficiency here to lower coupling factors for the agarose bound TEMPO compared to dissolved TEMPO.

There are two possible causes for the decrease in the coupling factor: (1) a change in the diffusion coefficient of the radical or water, or (2) a change in the distance of closest approach between the radical and the proton being hyperpolarized. Because the radicals are immobilized on the gels, the diffusion coefficient of the radicals is definitely affected, as is also evident from the line broadening of the ESR spectrum. The mobility of the water within the gel and in direct contact with bound radicals will also be reduced by the confines of the polymer network. However, because the diffusion coefficient of the radical is almost negligible compared to the diffusion coefficient of the water and the coupling factor is proportional to the sum of the two, the change of the diffusion coefficient of the faster water species has the dominant effect on the coupling factor. Therefore, in order to achieve the same enhancement for the bound TEMPO compared to a TEMPO solution, the mobility of the water within the vicinity of the bound radical must closely approach solution dynamics. This means that gels or other polymer matrices must be developed with functional groups that are fully solvated and allow for higher mobility for the local water as opposed to aiming for immobilized radicals that approach the mobility of dissolved radicals.

2.3. Flow polarization properties

We tested the continuous-flow mode Overhauser enhancement of ^{1}H water through our spin labeled gel material. The gels were loaded into a quartz reactor tube (2 mm OD, 1 mm ID) and centered in a 9.8 GHz ESR microwave cavity (Bruker Biospin, Billerica) at 0.35 T (Fig. 3). A syringe pump was used to flow HPLC grade water through the spin-labeled packing, then down stream to a home built probe tuned to 14.8 MHz for NMR detection (Fig. 3). When the microwave irradiation is turned off water flows from the ESR cavity to the NMR coil, where thermal polarization is detected. When microwave irradiation, resonant with an ESR transition of TEMPO, is turned on, hyperpolarization is initiated for the ^{1}H signal of water in contact with the spin labeled gel and NMR signal with an altered amplitude and phase is observed (Fig. 4, top). Over an observation time of 2 min we switched the microwave on and off to show that we could create contrasted signals through the control of microwave irradiation (Fig. 4, bottom). A comparison of the enhancements observed for static and flowing water over each matrix can be seen in Table 1.

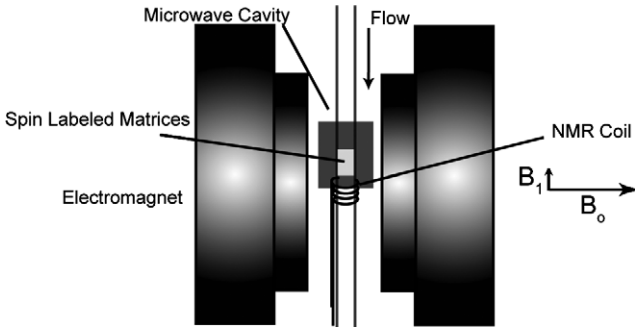

Fig. 3. Water was pumped though a flow cell containing the spin-labeled polarization matrix for continuous DNP polarization inside the microwave cavity placed in an electromagnet. The hyperpolarized water flows downstream for NMR detection using a home built probe.

To test for radical leakage into the polarized fluids we collected one liter of water flowing through the spin-labeled agarose gel, concentrated it to 1 mL, and then measured its EPR spectrum to reveal no detectable radical signature. From the detection limits of our instrument we can make a conservative estimate of less than 1 nM radical is leaching out of the matrix.

Polarization build up time is an important factor when considering the flow rate through the polarization matrix. Assuming that the electron spin saturation is much faster than the nuclear T_1, the hyperpolarization build-up will be dependent on the T_1 of the nucleus to be polarized [5,19].

$$E = 1 - fs\rho\frac{\gamma_S}{\gamma_I}(1 - e^{-t/T_1}) \quad (4)$$

The T_1 of TEMPO loaded agarose is 140 ms, so to achieve 95% polarization in the matrix the water must reside within the gel for 420 ms. In our experiment the water transits the gel matrix in 300 ms resulting in 90% of the polarization build up, corresponding to $E = -29$. There will also be additional loss of polarization due to

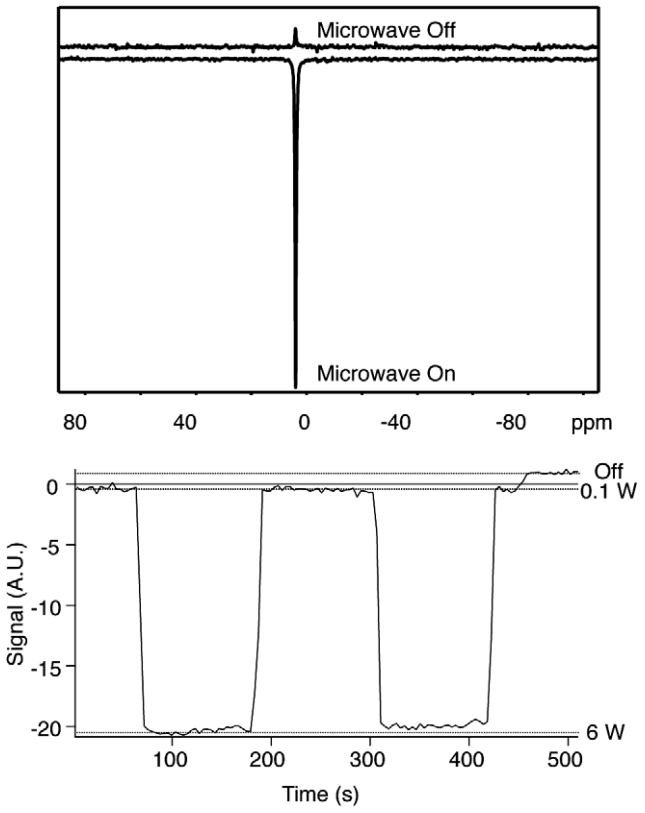

Fig. 4. Upon microwave irradiation on resonant of the radical's EPR transition, the ^{1}H NMR signal of water is negatively enhanced, which returns to the equilibrium value after the microwave irradiation was turned off (top). An event plot (bottom) shows how NMR contrast of water can be turned on or off although the physically identical water is flowing through the NMR probe with time.

T_1 relaxation as the radical free water travels from the polarization matrix to the detection coil. Given that the T_1 of the radical-free water is 3.0 s and the flow transit between polarization chamber and detection is 0.6 s, spin–lattice relaxation in the time it takes the water to travel from the polarization site to the NMR detection coil results in a final hyperpolarization of $E = -24$.

We measured the flowing DNP enhancement of a 10 mM solution of 4-amino-TEMPO and found the enhancement to be −42. This value is larger than that measured for the gels, however the sample still contains 10 mM radical, which will broaden NMR lines, reduce the T_1 of the water, and is potentially toxic to *in vivo* and biological samples. The signal has also decayed much more over the short transit time than the radical free water produced from spin labeled gels.

Overall, our studies reveal that sufficiently high radical loading (C), water access to these radicals (f), high mobility of water (ρ), and direct (close) contact between the radicals and protons (ρ) are necessary to provide an optimal DNP polarization medium. Therefore, a water permeable gel network with large pores, high mobility, yet good mechanical stability needs to be developed to fully exploit the Overhauser effect for continuous-flow polarization of radical-free fluids. So far, our spin labeled agarose media offers the best Overhauser performance reported without leaking radicals into the hyperpolarized fluids.

3. Conclusions

The steady-state infusion of non-toxic or physiologically native molecules as contrast agents, by hyperpolarizing their magnetic spin states, possesses great potential for *in vivo* and biological applications of MRI because they provide high contrast and are biocompatible. The Overhauser effect is an advantageous technique for signal enhancement because fluid-phase DNP is efficient at magnetic fields that are relevant for MRI (0.35–1 T). By immobilizing the free radical TEMPO onto gel chromatography materials, we created a polarization medium that satisfies the needs for efficient transient DNP as well as radical-free steady-state injection and detection. Cross-linked agarose or other porous and permeable gel materials appear to be good media for polarizing biological samples because their large pores and disperse chains allow for high concentration and considerable mobility of the radicals and solvent, and the hydrophilic nature of the gel provides for good dispersion of the radicals in the water medium. By further enhancing the fluid's mobility within the pores, we hope to maximize the Overhauser-driven DNP enhancement. For TEMPO-based spin labels, we expect to be able to reach ^{1}H enhancements of about −120-fold, corresponding to ^{1}H thermal polarization of a 45 T field.

4. Experimental

TEMPO covalently immobilized on silica gel was purchased from Sigma–Aldrich. The silica gel grain size was 120–230 mesh with a 60 Å mean pore size. The radical loading was 0.7 mmol/g, which we estimate to be a nominal concentration of 900 mM when fully exposed to water.

4.1. Synthesis of ^{15}N-perdeutero-4-amino-2,2,6,6-tetramethylpypiridine-1-oxyl

^{15}N-perdeuterated-4-amino-TEMPO was synthesized utilizing several previously published methods[14], [20-24] (Scheme 1). All isotopically enriched reagents and solvents were purchased from Cambidge Isotopes Laboratory and Isotec.

4.2. Acetonin(**1**) and triacetoneamine(**1b**)

Acetonin (**1**) was synthesized from ^{15}N-ammonia and d_6-acetone, using ^{15}N ammonium chloride as a catalyst and potassium iodide as a promoter. ^{15}N-ammonium chloride (0.65 g, 12 mmol) and potassium idodide (0.1 mg, 1.3 mmol) were mixed with 6 mL of d_6-acetone (4.62 g, 72 mmol) in a three neck flask fitted with a gas inlet and dry ice condenser, then ammonia (1.3 g, 72 mmol) was bubbled though the acetone over 4 h to create acetonin. As the ammonia reacted, a light yellow oil appeared at

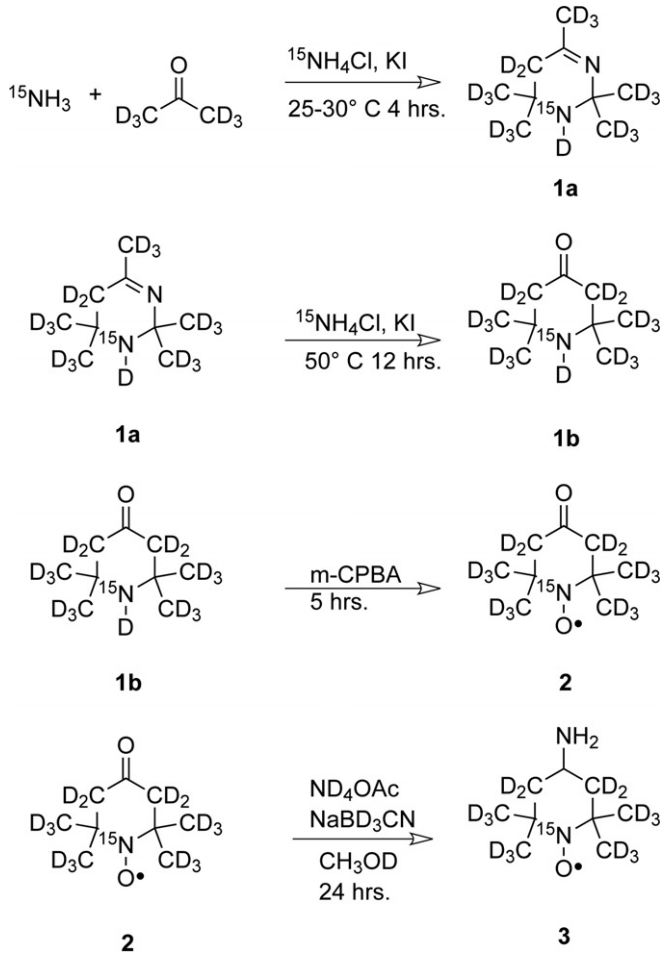

Scheme 1.

the surface. The dry ice condenser was then replaced with a reflux condenser and another 6 mL of d_6-acetone and 1 mL of deuterium oxide was added to the mixture. The reaction was then heated at 50 °C for another 12 h to convert the acetonin to ^{15}N-perdeutero-triacetoneamine (**1b**). After reacting for several hours, the solution turns deep red. The acetone was removed *in vacuo*, and then mixed with 17.5 mL of NaOD while stirring vigorously. This mixture was extracted three times with anhydrous diethyl ether and dried over $MgSO_4$. The ether was then removed *in vacuo* and the product recrystalized from ~5 mL of CCl_4 three times to yield 5.5 g of long yellow crystals. The crystals were dried overnight in a vacuum desiccator, and then stored at 4 °C until they were used in the next step.

4.3. ^{15}N-perdeutero-4-oxo-TEMPO (*2*)

Triacetoneamine (**1b**) was oxidized to ^{15}N-perdeutero-4-oxo-TEMPO (**2**) with meta-chloroperbenzoic acid. To 90% concentrated triacetoneamine (5.5 g, 28 mmol) dissolved in 75 mL of chloroform, 77% meta-chloroperbenzoic acid (m-CPBA) (14.3 g, 64 mmol) was added over 1 h, and then further reacted for another 5 h at room temperature. As the m-CPBA was added to the mixture, the reaction product became thick and a yellow oil formed at the top. The crude product was chromatographically purified on neutral alumina eluting with methylene chloride. Fractions containing the product were pooled and the solvent was removed to yield 3.6 g of oil.

4.4. ^{15}N-perdeutero-4-amino-TEMPO (*3*)

^{15}N-perdeutero-4-oxo-TEMPO (**2**) was reductively aminated using sodium cyanoborodeuteride to produce ^{15}N-perdeutero-4-amino-TEMPO (**3**). The ^{15}N-perdeutero-4-oxo-TEMPO oil (3.6 g) was added to a solution of ~90% ND_4OAc (13.7 g, 0.16 mol) dissolved in 50 mL of methan-D-ol. Molecular sieves 3A (8 g) were used to absorb water. $NaBD_3CN$ (0.79 g, 12 mmol) was then added and stirred for 24 h. The reaction was then filtered and the solvent was removed *in vacuo*. The resulting oil was resuspended in a minimal amount of deuterium oxide; the pH was reduced to 5–6 with dilute deuterium chloride, and extracted three times with $CDCl_3$. The solution was then made alkaline with sodium deuteroxide and extracted with $CHCl_3$. The organic was collected, dried over $MgSO_4$, and removed *in vacuo*. Residual solvent was finally distilled off to yield 1.6 g of final product. ND_4OAc was created by dissolving NH_4OAc in MeOD and evaporating off the solvent three times.

4.5. Immobilization of radicals

NHS-Sepharose 4 Fast Flow was purchased from Sigma–Aldrich. The free radical was attached to 45–165 μM diameter NHS-Sepharose 4 Fast Flow beads (GE Healthcare), as described previously[12], by reacting the *N*-hydroxysuccinimide ester reactive group of the Sepharose with the amine of 4-amino-TEMPO to produce a stable peptide bond as shown in Scheme 2. 4-amino-TEMPO (75 mg) was dissolved in 0.5 mL of coupling buffer (0.2 M $NaHCO_3$, 0.5 M NaCl, pH 8.3). The NHS-Sepharose was washed with 1 mM HCl 10 times at 4 °C. The TEMPO solution was added to the Sepharose and shaken overnight at 4 °C. After reacting, excess 4-amino-TEMPO was washed from the Sepharose with water. The gel was labeled to the maximum capacity, which we estimate to be 10 mM 4-amino-TEMPO. The labeled Sepharose was stored in 30% ethanol.

4.6. DNP-enhanced NMR spectroscopy

Static DNP-enhanced NMR experiments were carried out using a cw X-band ESR instrument and equal conditions as described above. A home-built U-shape NMR coil made of 0.013″ diameter silver wire (Teflon coated) was introduced into a TE_{102} square ESR cavity. The coil is connected via twisted wires and coaxial cable to a simple LC tuning box tuned to 14.8 MHz and connected to a broadband channel of a Bruker Avance NMR spectrometer. During DNP operation, the ESR cavity stays tuned at a

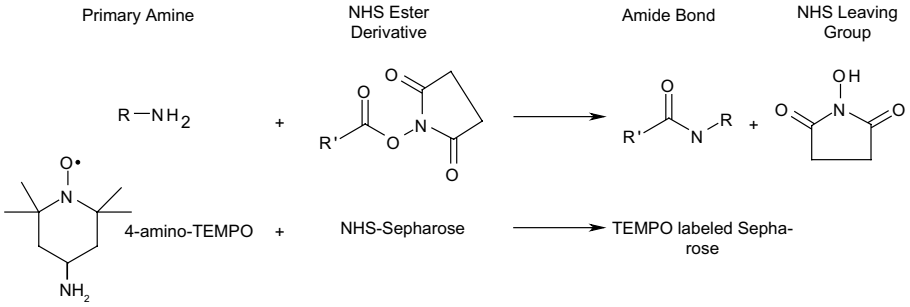

Scheme 2.

quality factor (Q) of about 1000–2000 and irradiates the unpaired electrons with a power output up to 6 W from a custom microwave source. The flow experiments were carried out in a flow tube and NMR signal was detected with a solenoid coil (Fig. 1).

Due to the dielectric properties of water, we observe sample heating (~50 °C) in static samples under high power microwave irradiation (6 W). Such heating will decrease the viscosity of the water and increase the coupling factor and ultimately increase the observed enhancement. Heating effects can be kept minimal by flowing air over the sample and using somewhat lower power (>2.5 W). However, because we are performing DNP on flowing water through the microwave cavity we expect the heating effect to be insignificant for the flow measurements, and therefore do not expect to observe any increase in enhancement.

4.7. Determination of E_{max}

The maximum enhancement ($E_{\max}$) was experimentally determined for each sample as describe here. First, an ESR spectrum is recorded to determine the frequency and field at which one of the ESR lines of the nitroxide spin labels should be irradiated. Then, the amplified NMR spectra are recorded with on resonant ESR irradiation at varying microwave B_1 field strengths (Fig. 2). The enhancement is computed relative to the NMR spectrum without microwave irradiation, and the enhancement factor plotted against power (P). Eq. (5) represents a modified version of Eq. (1), where $1/n[\alpha P/(1+\alpha P)]$ corresponds to the saturation factor, s.

$$E = 1 - \rho f \frac{1}{n}\left[\frac{\alpha P}{1+\alpha P}\right]\frac{\gamma_S}{\gamma_I} \tag{5}$$

The number of hyperfine split lines, n, is 2 or 3 for the spin probes used, and α is a numerical factor. γ_S/γ_I is the ratio between the gyromagnetic ratio of the unpaired electron versus the protons, thus 680. The maximum enhancement can be computed in the limit of infinite power.

Acknowledgments

The authors thank M. Marsini and T. Petus for help, guidance, and resources while synthesizing perdeutero-^{15}N-4-amino-TEMPO. Also, continuous discussions with Brandon Armstrong about DNP theory and hardware development of Mark Lingwood and Brandon Armstrong were important contributions to this work. This work was partially supported by the Materials Research Laboratory program of the National Science Foundation (DMR00-80034), the Institute for Collaborative Biotechnologies (DAAD19-03-D-0004) from the U.S. Army Research Office, the Petroleum Research Funds (PRF#45861-G9) of the American Chemical Society and the Faculty Early CAREER Award (20070057) of the National Science Foundation.

References

[1] A.W. Overhauser, Polarization of nuclei in metals, Phys. Rev. 92 (1953) 411–415.
[2] D.A. Hall, D.C. Maus, G.J. Gerfen, S.J. Inati, L.R. Becerra, F.W. Dahlquist, R.G. Griffin, Polarization-enhanced NMR spectroscopy of biomolecules in frozen solution, Science 276 (1997) 930–932.
[3] R.A. Wind, J.H. Ardenkjaer-Larsen, H-1 DNP at 1.4 T of water doped with a triarylmethyl-based radical, J. Magn. Reson. 141 (1999) 347–354.
[4] V.S. Bajaj, M.K. Hornstein, K.E. Kreischer, J.R. Sirigiri, P.P. Woskov, M.L. Mak-Jurkauskas, J. Herzfeld, R.J. Temkin, R.G. Griffin, 250 GHz CW Gyrotron Oscillator for Dynamic Nuclear Polarization in Biological Solid State NMR, J. Magn. Reson. 189 (2007) 251–279.
[5] K.H. Hausser, D. Stehlik, Dynamic nuclear polarization in liquids, Adv. Magn. Reson. 3 (1968) 79–139.
[6] R. Gitti, C. Wild, C. Tsiao, K. Zimmer, T.E. Glass, H.C. Dorn, Solid-liquid intermolecular transfer of dynamic nuclear polarization. Enhanced flowing fluid proton NMR signals via immobilized spin labels, J. Am. Chem. Soc. 110 (1988) 2294–2296.
[7] H.C. Dorn, T.E. Glass, R. Gitti, K.H. Tsai, Transfer of 1H and 13C dynamic nuclear polarization from immobilized nitroxide radicals to flowing liquids, Appl. Magn. Reson. 2 (1991) 9.
[8] N.M. Loening, M. Rosay, V. Weis, R.G. Griffin, Solution-state dynamic nuclear polarization at high magnetic field, J. Am. Chem. Soc. 124 (2002) 8808–8809.
[9] J.H. Ardenkjaer-Larsen, B. Fridlund, A. Gram, G. Hansson, L. Hansson, M.H. Lerche, R. Servin, M. Thaning, K. Golman, Increase in signal-to-noise ratio of >10,000 times in liquid-state NMR, Proc. Natl. Acad. Sci. USA 100 (2003) 10158–10163.
[10] E. Johansson, S. Månsson, R. Wirestam, J. Svensson, J.S. Petersson, K. Golman, F. Ståhlberg, Cerebral perfusion assessment by bolus tracking using hyperpolarized 13C, Magn. Reson. Med. 51 (2004) 464–472.
[11] C.-G. Joo, K.-N. Hu, J.A. Bryant, R.G. Griffin, In situ temperature jump high-frequency dynamic nuclear polarization experiments:

enhanced sensitivity in liquid-state NMR spectroscopy, J. Am. Chem. Soc. 128 (2006) 9428–9432.
[12] E.R. McCarney, B.D. Armstrong, M.D. Lingwood, S. Han, Hyperpolarized water as an authentic magnetic resonance imaging contrast agent, Proc. Natl. Acad. Sci. USA 104 (2007) 1754–1759.
[13] H.C. Dorn, J. Wang, L. Allen, D. Sweeney, T.E. Glass, Flow dynamic nuclear polarization, a novel method for enhancing NMR signals in flowing fluids, J. Magn. Reson. (1969) 79 (1988) 404–412.
[14] B.D. Armstrong, S. Han, A new model for Overhauser enhanced nuclear magnetic resonance using nitroxide radicals, J. Chem. Phys. 127 (2007). Article 104508.
[15] A. Abragam, M. Borghini, Dynamic polarization of nuclear targets. Progr, in: C.J. Gorter (Ed.), Low Temp. Phys. North-Holland 4 (1964) pp. 384–449.
[16] I. Nicholson, D.J. Lurie, F.J.L. Robb, The application of proton–electron double-resonance imaging techniques to proton mobility studies, J. Magn. Reson. B 104 (1994) 250–255.
[17] R.D. Bates, W.S. Drozdoski, Use of nitroxide spin labels in studies of solvent–solute interactions, J. Chem. Phys. 67 (1977) 4038–4044.
[18] B.H. Robinson, D.A. Haas, C. Mailer, Molecular-dynamics in liquids—spin–lattice relaxation of nitroxide spin labels, Science 263 (1994) 490–493.
[19] I. Solomon, Relaxation processes in a system of 2 spins, Phys. Rev. 99 (1955) 559–565.